Journal of Biomolecular NMR **29:** 309–318, 2004.

Quantification of H/D isotope effects on protein hydrogen-bonds by $^{h3}J_{NC'}$ and $^{1}J_{NC'}$ couplings and peptide group ^{15}N and $^{13}C'$ chemical shifts

Victor A. Jaravine, Florence Cordier & Stephan Grzesiek*
Division of Structural Biology, Biozentrum der Universität Basel, Klingelbergstrasse 70, CH-4056 Basel, Switzerland

Received 4 December 2003; Accepted 12 January 2004

Key words: hydrogen-deuterium exchange, protein structure, protein stability, hydrogen bond stability, Ubbelohde effect, NMR

Abstract

The effect of hydrogen/deuterium exchange on protein hydrogen bond coupling constants $^{h3}J_{NC'}$ has been investigated in the small globular protein ubiquitin. The couplings across deuterated or protonated hydrogen bonds were measured by a long-range quantitative HA(CACO)NCO experiment. The analysis is combined with a determination of the H^N/D^N isotope effect on the amide group $^{1}J_{NC'}$ couplings and the ^{15}N and $^{13}C'$ chemical shifts. On average, H-bond deuteration exchange weakens $^{h3}J_{NC'}$ and strengthens $^{1}J_{NC'}$ couplings. A correlation is found between the size of the ^{15}N isotope shift, the ^{15}N chemical shift, and the $^{h3}J_{NC'}$ coupling constants. The data are consistent with a reduction of donor-acceptor overlap as expected from the classical Ubbelohde effect and the common understanding that H^N/D^N exchange leads to a shortening of the N-hydron bond length.

Abbreviations: H-bond – hydrogen bond.

Introduction

Isotopic replacement of hydrogen (^{1}H) by deuterium (^{2}H) or tritium (^{3}H) in either solute or solvent molecules is a common technique for the study of biomacromolecules. Such experiments include the detection of the exchange of labile hydrogen nuclei in proteins or nucleic acids (Hvidt and Nielsen, 1966; Englander et al., 1996; Englander et al., 2003), contrast variations and increase of scattering densities in neutron diffraction techniques (Shu et al., 2000), the use of $^{2}H_2O$ as a frequency standard or means to eliminate unwanted $^{1}H_2O$ signals in high resolution NMR, and the deuteration of biomacromolecules in order to reduce NMR magnetization losses (Markley et al., 1968; LeMaster and Richards, 1988; Torchia et al., 1988; Grzesiek et al., 1993; Rosen et al., 1996; Salzmann et al., 2000).

Usually it is assumed that the macromolecular structure remains very similar, regardless of whether intrinsic hydrogen nuclei are substituted or whether the molecules are dissolved in water of varying hydrogen isotope content. Yet sometimes considerable kinetic and thermodynamic hydrogen isotope effects are observable in such systems. E.g., an up to nine-fold increase of the catalysis rate of amino acid oxidase was found when a deuterated substrate was used (Harris et al., 2001). Increases in transition temperature on the order of several degrees and decreases in the unfolding enthalpy of about 15 kcal/mol due to deuteration of protein and solvent were observed in a study of several proteins (Makhatadze et al., 1995). However, such large enthalpy changes were found to be mostly compensated for by entropic changes of similar size, which result from the different hydration of proteins in D_2O and H_2O. A recent study on kinetic H/D amide isotope effects (Krantz et al., 2002) concluded that protonated helical H-bonds are stabilized by 9 cal/mol/site as compared to deuterated H-bonds, whereas no such isotope effects were observed for β-sheet H-bonds.

Structural changes within macromolecules upon deuteration are clearly much less pronounced than the kinetic and thermodynamic effects. The structural effects are commonly described in terms of changes

*To whom correspondence should be addressed. E-mail: Stephan.Grzesiek@unibas.ch

in bond vibrations. The lower zero-point vibrational energy of deuterated compounds together with the anharmonicities of bond potentials leads to a shortening of covalent D-X bonds on the order of few hundredths of one Angstroem as compared to H-X bonds (Jameson, 1996; Benedict et al., 1998). This effect manifests itself clearly in NMR as chemical shift changes of neighboring nuclei, e.g. the well-described one-bond isotope shift of the X-nucleus (Hansen, 1988; Jameson, 1996). In a addition, a recent solid state NMR study gave more direct evidence for the deuterium-induced covalent bond shortening based on dipolar couplings (Benedict et al., 1998). Changes in bond angles on the order of less than 0.5° have been reported as a result of methyl group deuteration (Mittermaier and Kay, 2002).

For hydrogen bonds (H-bonds) the shortening of the covalent bond length upon deuteration is usually accompanied by a change of the donor-acceptor distance of similar order. A lengthening of the donor-acceptor distance upon deuteration is known as the classical Ubbelohde effect (Ubbelohde and Gallagher, 1955; Smirnov et al., 1996; Benedict et al., 1998), which has been observed in many X-ray crystallographic studies of small molecules (e.g., Ubbelohde and Gallagher, 1955; Kreevoy and Young, 1999). However, gas-phase studies show that also shortening of the donor-acceptor distance can occur due to a coupling of bending and stretching modes (Legon and Millen, 1988; Sokolov and Savel'ev, 1994). Very little is known about such Ubbelohde effects in biomacromolecules.

Scalar couplings across H-bonds (Dingley and Grzesiek, 1998; Pervushin et al., 1998; Shenderovich et al., 1998; Cordier and Grzesiek, 1999; Cornilescu et al., 1999a) have been shown to have a strong dependence on the H-bond donor-acceptor distances (Dingley and Grzesiek, 1998; Cordier and Grzesiek, 1999; Cornilescu et al., 1999b). This finding can be rationalized by a simplified LCAO-MO Sum-over-States analysis of H-bond moieties, which shows that the H-bond couplings depend to a first approximation on the square of the resonance integrals between the hydrogen and the acceptor orbitals and hence on their overlap (Barfield et al., 2001). Thus H-bond couplings provide a measure for the overlap of hydrogen and acceptor atoms.

A recent study on a limited number of H-bonds in selectively labeled double-stranded DNA reported the weakening of H-bond $^{h2}J_{NN}$ couplings after H_2O/D_2O solvent exchange (Kojima et al., 2000). In the present work, we have systematically investigated the effect of hydrogen/deuterium exchange on protein H-bond coupling constants $^{h3}J_{NC'}$ in the small globular protein ubiquitin. We combine this analysis with a determination of the hydrogen/deuterium isotope effect on the ^{15}N, $^{13}C'$, and $^{1}H^{\alpha}$ chemical shifts as well as on the one-bond $^{1}J_{NC'}$ couplings, which have been shown to be dependent on the strength of both peptide group, i.e. carbonyl and amide, H-bonds (Juranic and Macura, 2001). The data show that deuteration of protein backbone H-bonds leads to a slight average decrease of $|^{h3}J_{NC'}|$, an increase of $|^{1}J_{NC'}|$, and a decrease in the chemical shift, i.e. an increase in the shielding for ^{15}N and $^{13}C'$. This is consistent with a reduction of H-bond donor-acceptor overlap, a shortening of the length and an increase of electron density in the N-hydron bond.

Materials and methods

$^{h3}J_{NC'}$ *couplings*

The pulse scheme of the HA(CACO)NCO experiment used to quantify $^{h3}J_{NC'}$ coupling constants in deuterated protein H-bonds is shown in Figure 1. In order to observe the $^{h3}J_{NC'}$ correlations after amide proton/deuteron exchange via the H^{α} protons, the $H^{N} \rightarrow N$ out-and-back INEPT transfer of the original quantitative H-bond HNCO experiment (Cordier and Grzesiek, 1999) is substituted by a sequence of three out-and-back INEPT transfers ($H^{\alpha} \rightarrow C^{\alpha}$, $C^{\alpha} \rightarrow C'$, and $C' \rightarrow N$) at the beginning (points a-b) and end (points c-d) of the sequence. Similar to the original quantitative HNCO, the scheme of Figure 1 is carried out twice. For the first experiment (A), the 180° $^{13}C'$ pulses are set close ($\Delta_4 \approx 0$, Figure 1) to the refocusing 180° ^{15}N pulses in the middle of the 100 ms-long (2T) $N \rightarrow C'$ transfer intervals. In this case, sequential $^{1}J_{NC'}$ couplings (~ -15 Hz) are approximately refocused, but transfer via the smaller $^{h3}J_{NC'}$ couplings is achieved. For the second experiment (B), the 180° $^{13}C'$ pulses are shifted ($\Delta_4 = 16.5$ ms, Figure 1) such that transfer by $^{1}J_{NC'}$ is optimized. The absolute size of the $^{h3}J_{NC'}$ coupling constants can then be determined to a good approximation from the intensity ratio of the H-bond cross peak (A) and the sequential cross peak (B): $|^{h3}J_{NC'}| \approx 1/(2\pi T)\ \mathrm{atan}^{-1}((I_A/I_B)^{1/2})$ (Cordier and Grzesiek, 1999). Based on experimental evidence (Cornilescu et al., 1999b) and theoretical predictions (Scheurer and Brüschweiler, 1999), $^{h3}J_{NC'}$ is assumed to be negative in the following.

The experiment was carried out on two 300 µl aqueous samples of uniformly $^{15}N/^{13}C$-labeled 10 mM

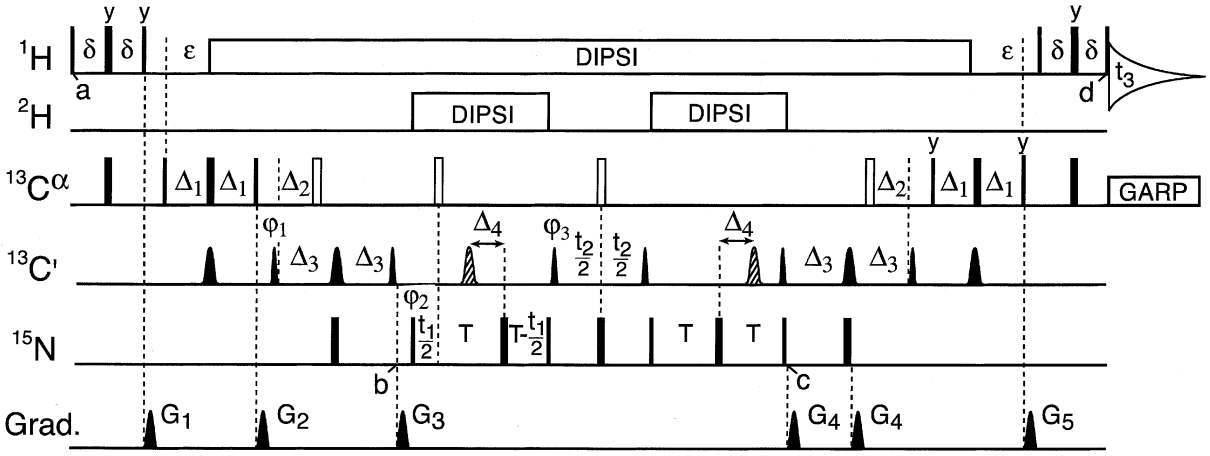

Figure 1. Pulse scheme of the HA(CACO)NCO experiment used to detect $^{h3}J_{NC'}$ connectivities in the case of deuterated backbone H-bonds of proteins. Narrow and wide bars correspond to rectangular 90° and 180° pulses, respectively. All pulse phases are x, unless specified otherwise. ^{1}H rectangular pulses are applied at an RF field strength of 31 kHz (carrier at 8.0 ppm, RF field strengths are indicated for the experiment carried out at 800 MHz). ^{1}H DIPSI decoupling was carried out with an RF field strength of 6.3 kHz. ^{2}H DIPSI decoupling (carrier at 8 ppm) was carried out with an RF field strength of 0.7 kHz. DIPSI decoupling was interrupted during the application of pulse field gradients. The 90° and 180° $^{13}C^{\alpha}$ pulses denoted by filled rectangles are applied (carrier at 56 ppm) with an RF-strength of 6.3 and 14.0 kHz, respectively, such that they have a null in their excitation profile at the carbonyl $^{13}C'$ frequencies. The $^{13}C^{\alpha}$ 180° pulses denoted by open rectangles are applied with an RF-strength of 6.3 kHz. GARP $^{13}C^{\alpha}$ decoupling (3.33 kHz) was carried out during ^{1}H detection (t_3). $^{13}C'$ pulses (carrier at 177 ppm) have the shape of the center lobe of a sinc-function and durations of 0.22 ms (180°) and 0.11 ms (90°). ^{15}N rectangular pulses are applied at 116.5 ppm with an RF field strength of 6.4 kHz. Delay durations: $\delta = 1.5$ ms, $\varepsilon = 3.5$ ms, $T = 50$ ms, $\Delta_1 = 3.7$ ms, $\Delta_2 = 4.5$ ms, $\Delta_3 = 12$ ms. As described in the text, the hatched 180° $^{13}C'$ pulses are shifted between two positions ($\Delta_4 = 10$ μs or 16.5 ms) to obtain cross and reference spectra, respectively. Phase cycling: $\varphi_1 = 2x, 2(-x)$; $\varphi_2 = 4x, 4(-x)$; $\varphi_3 = x, -x$; receiver $= -x, x, x, -x, x, -x, -x, x$. Quadrature detection in the t_1, t_2 dimensions is obtained by States-TPPI phase incrementation of φ_2 and φ_3. Pulsed field gradients are sine-bell-shaped, with peak amplitudes of 30 G/cm at the center and durations (directions) $G_{1,2,3,4,5} = 5.0$ (x), 0.55 (z), 0.55 (y), 0.8 (y), and 1.6 (x) ms.

ubiquitin at pH* 7 (uncorrected meter reading), 35 °C. The hydrogen isotope composition of the water was either 95%/5% or 1%/99% H_2O/D_2O. The exchange of water between the two conditions was achieved by dialysis in Centricon-3 tubes (Amicon). In order to ensure complete exchange of ubiquitin amide hydrogens with the solvent for these and all other samples, the pH* was temporarily raised to 9, the samples were then equilibrated under this condition at 50 °C overnight, and the pH* was subsequently restored to 7. Data were collected on a Bruker DRX-800 spectrometer, equipped with a triple resonance, 3-axis pulsed field gradient probe. For both sample conditions, spectra were recorded as 50* ($^{13}C'$) × 90* (^{15}N) × 384* ($^1H^{\alpha}$) complex data matrices with acquisition times of 22.5, 54, and 40 ms, respectively. The total experimental times for the H-bond (A) and reference (B) experiments were 40 and 20 h. In order to obtain estimates of the statistical errors of the coupling constants, experiments were carried out twice and the reported $^{h3}J_{NC'}$ values refer to mean and standard deviations from these two independent determinations.

$^1J_{NC'}$ *couplings*

Figure 2 shows the pulse scheme of the quantitative HA(CA)CO(N) experiment suitable for determination of $^1J_{NC'}$ coupling constants in proteins with deuterated amide hydrogen positions. The pulse sequence is deduced from the HACACO experiment (Ikura et al., 1990). The magnetization originates on H^{α} protons and after two INEPT transfers ($H^{\alpha} \rightarrow C^{\alpha}$, $C^{\alpha} \rightarrow C'$), $^{13}C'$ frequency labeling is achieved in a constant-time evolution period between points b and c. In the spirit of quantitative J-correlation (Bax et al., 1994), the experiment is also carried out once (A) with the 180° ^{15}N pulse used as a decoupling pulse ($\Delta_2 \approx 0$) and once (B) as a coupling pulse ($\Delta_2 = T$). The absolute value $^1J_{NC'}$ is then deduced from the intensity ratio of the two experiments as $|^1J_{NC'}| = 1/(2\pi T)\cos^{-1}(I_B/I_A)$, and $^1J_{NC'}$ is assumed as negative (Cornilescu et al., 1999b) in the following.

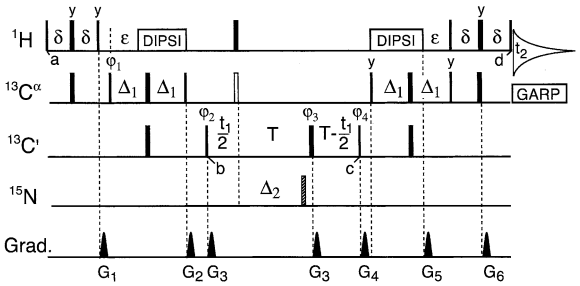

Figure 2. Pulse scheme of the HA(CA)CO(N) experiment used to determine $^1J_{NC'}$ coupling constants. Narrow and wide bars correspond to rectangular 90° and 180° pulses, respectively. All pulse phases are x, unless specified otherwise. ^{1}H rectangular pulses are applied at an RF field strength of 37 kHz, the carrier is centered on the water resonance (RF field strengths are indicated for the experiment carried out at 600 MHz). ^{1}H DIPSI decoupling was carried out with an RF field strength of 5 kHz. The filled 90° and filled (open) 180° $^{13}C^\alpha$ rectangular pulses, carrier at 56 ppm, are applied with an RF-strength of 4.7 and 10.5 (4.7) kHz, respectively, such that they have a null in their excitation profile at the carbonyl $^{13}C'$ frequencies. GARP $^{13}C^\alpha$ decoupling (3.1 kHz) was carried out during ^{1}H detection (t_2). $^{13}C'$ pulses (carrier at 177 ppm) were applied at an RF field strength of 4.7 kHz. ^{15}N rectangular pulses are applied at 116.5 ppm with an RF field strength of 6.25 kHz. Delay durations: $\delta = 1.5$ ms, $\varepsilon = 3.5$ ms, $T = 16.5$ ms, $\Delta_1 = 3.7$ ms, $\Delta_2 = 16.2$ ms (attenuated) or 10 μs (reference). Phase cycling: $\varphi_1 = x,-x$, $\varphi_2 = 2x, 2(-x)$, $\varphi_3 = 8x, 8y$, $\varphi_4 = 4x, 4(-x)$, receiver = R, −R, −R, R, with R = x, −x, −x, x. Quadrature detection in the t_1 dimension is obtained by States-TPPI phase incrementation of φ_2. Gradient durations (directions) $G_{1,2,3,4,5,6} = 5.0$ (−z), 2.15 (z), 0.7 (y), 2.15 (x), 1.6 (−z), 0.4023 (z) ms.

The HA(CA)CO(N) experiments were carried out on a Bruker DRX-600 spectrometer, equipped with a triple resonance, 3-axis pulsed field gradient probe. Spectra were recorded as 52* ($^{13}C'$) × 384* ($^1H^\alpha$) complex data 2D matrices with acquisition times of 31.2 and 63.9 ms, respectively. The experimental time for each of the two experiments was 4 hours. In order to obtain estimates of the statistical errors, each experiment was carried out twice.

The $^2H^N/^1H^N$ isotope effect on the $^1J_{NC'}$ coupling constants was determined by measuring the $^1J_{NC'}$ couplings on two 300 μl aqueous samples of uniformly $^{15}N/^{13}C$-labeled 2 mM ubiquitin at pH* 7, at 35 °C with a water hydrogen isotope composition of either 95%/5% or 1%/99%. The isotope effect $\Delta^1J_{NC'}(^{2/1}H^N)$ was then calculated as the difference of the $^1J_{NC'}$ coupling of the heavier minus the lighter isotopomer.

$^1\Delta^{15}N(^{2/1}H^N)$, $^2\Delta^{13}C'(^{2/1}H^N)$, *and* $^4\Delta^1H^\alpha(^{2/1}H)$ *isotope shifts*

Intraresidue one-bond isotope shifts on amide ^{15}N nuclei, $^1\Delta^{15}N(^{2/1}H)$, interresidue two-bond isotope shifts on the carbonyl ^{13}C resonance, $^2\Delta^{13}C'$ ($^{2/1}H$), and interresidue four-bond isotope shifts on the $^1H^\alpha$ resonance, $^4\Delta^1H^\alpha(^{2/1}H)$, resulting from amide proton/deuteron substitution were determined by a 3D HA(CA)CON experiment (Wang et al., 1995). This experiment was performed on a 300 μl aqueous sample of uniformly $^{15}N/^{13}C$-labeled 2 mM ubiquitin in 50% H_2O/50% D_2O, at pH* 7, at 35 °C. Data were collected on a Bruker DRX-600 spectrometer, equipped with a triple resonance, 3-axis pulsed field gradient probe. The 3D data matrix consisted of 40* (^{13}C) × 100* (^{15}N) × 384* ($^1H^\alpha$) complex data points with acquisition times of 32, 120 and 51.1 ms, respectively. For the estimation of the statistical error, two identical experiments were recorded with total experimental times of 20 h each. For most amide groups except prolines, two individual HA(CA)CON crosspeaks with equal intensity could be observed resulting from deuterated or protonated amide groups. Following the convention introduced by Gombler (1982), the n-bond isotope shifts $^n\Delta X(^{2/1}H^N)$ were calculated as the difference of the ^{15}N, $^{13}C'$, or $^1H^\alpha$ chemical shifts of the crosspeak corresponding to the heavier isotopomer minus the respective values for the lighter isotopomer.

Results

$^{h3}J_{NC'}$ *couplings*

Figure 3 shows a strip plot of the results of the long-range HA(CACO)NCO carried out on the 1%/99% H_2O/D_2O ubiquitin sample. In total, 20 $^{h3}J_{NC'}$ connectivities could be observed via the deuterated H-bonds. Also visible are one intraresidue $^2J_{NC'}$ (I44) and a number of not completely suppressed sequential $^1J_{NC'}$ connectivities. The $^{h3}J_{NC'}$ couplings calculated from intensity ratios of cross-correlation peaks and the respective reference peaks yield values between −0.3 to −0.8 Hz (Table 1) for the deuterated H-bonds.

In order to compare these values to the protonated H-bonds, a second long-range HA(CACO)NCO experiment was carried out under identical conditions for the 95%/5% H_2O/D_2O ubiquitin sample. Due to the enhanced dipolar relaxation from the amide hydrogen nucleus in protonated H-bonds (Wang et al., 1995), the sensitivity on this sample was about 2–3 times weaker than for the D_2O sample. In this case, only ten $^{h3}J_{NC'}$ correlations could be observed

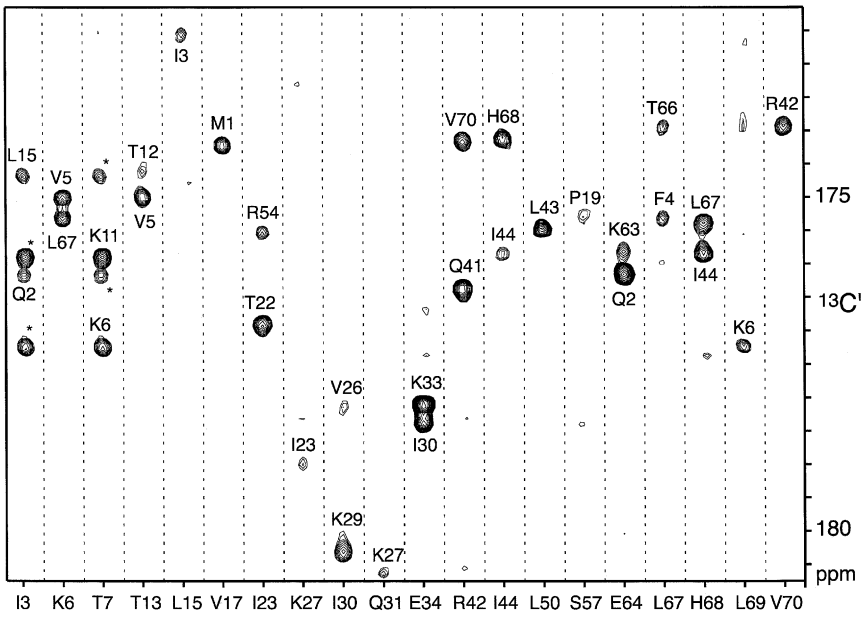

Figure 3. 3D HA(CACO)NCO spectrum showing through deuterated H-bond $^{h3}J_{NC'}$ connectivities for ubiquitin in 1%/99% H_2O/D_2O. Strips were extracted from the 3-dimensional data cube at the ^{15}N frequency of the H-bond donor residue and the $^{1}H^{\alpha}$ frequency of its preceding amino acid. The horizontal axis is labeled by the residue name of the H-bond donor. Resonances are labeled by the residue name of the correlated $^{13}C'$ atom. The spectrum was recorded with a total experimental time of 40 h.

(Table 1). Albeit there is a large scatter of the individual data points that is caused by the experimental noise and possibly true structural deviations, the absolute size of the $^{h3}J_{NC'}$ couplings in H_2O seems very slightly stronger than the corresponding couplings in D_2O (Figure 4A). The mean difference amounts to $<^{h3}J_{NC'}(H_2O$, HA(CACO)NCO) – $^{h3}J_{NC'}(D_2O$, HA(CACO)NCO)$> = -0.04 \pm 0.04$ Hz (N = 10).

A very similar result was obtained when the data were compared to $^{h3}J_{NC'}$ values derived from a long-range HNCO-TROSY experiment with amide proton detection in 95%/5% H_2O/D_2O (Table 1). Most of the $^{h3}J_{NC'}$-couplings in H_2O derived by the HNCO experiment have a slightly larger absolute size than the corresponding values in D_2O from the HA(CACO)NCO experiment (Figure 4B). The average difference $<^{h3}J_{NC'}(H_2O$, HNCO) – $^{h3}J_{NC'}(D_2O$, HA(CACO)NCO)$>$ amounts to a similar value of -0.03 ± 0.03 Hz (N = 20). Clearly, the latter comparison could be affected by possible systematic differences between the quantitative HA(CACO)NCO and the HNCO experiment. However, the agreement between the $^{h3}J_{NC'}$ values in H_2O obtained by the two schemes is quite reasonable: the average difference $<^{h3}J_{NC'}(H_2O$, HNCO) – $^{h3}J_{NC'}(H_2O$, HA(CACO)NCO)$>$ amounts to only -0.01 ± 0.03 Hz (N = 10) and no systematic deviations appear between the two data sets (Figure 4C). Hence, the analysis of all experiments is consistent with a very modest strengthening of 0.03 ± 0.03 Hz of the $^{h3}J_{NC'}$-interactions for protonated versus deuterated amide H-bonds.

The small change in the couplings should imply a small change in the overlap between the electronic orbital of the hydrogen and the acceptor oxygen in the protein H-bonds. To estimate this change in overlap, to a first approximation the empirical formula $\Delta r/Å = -1/4\ \Delta\ln|^{h3}J_{NC'}|$ (Cornilescu et al., 1999b; Cordier and Grzesiek, 2002) could be used for an assumed linear H-bond, where Δr indicates the change in hydrogen-acceptor distance. Thus, for $^{h3}J_{NC'}$-couplings of about -0.4 Hz, the difference of 0.03 ± 0.03 Hz of deuterated vs. protonated H-bonds would correspond to a change in the hydrogen-acceptor distance of 0.02 ± 0.02 Å.

$^{1}J_{NC'}$ *couplings*

A strong correlation between peptide group $^{1}J_{NC'}$ and H-bond $^{h3}J_{NC'}$ coupling constants has been reported by Juranic and Macura (2001), where a weakening of H-bonds and $^{h3}J_{NC'}$ couplings corresponds to a strengthening of the $^{1}J_{NC'}$ coupling constant:

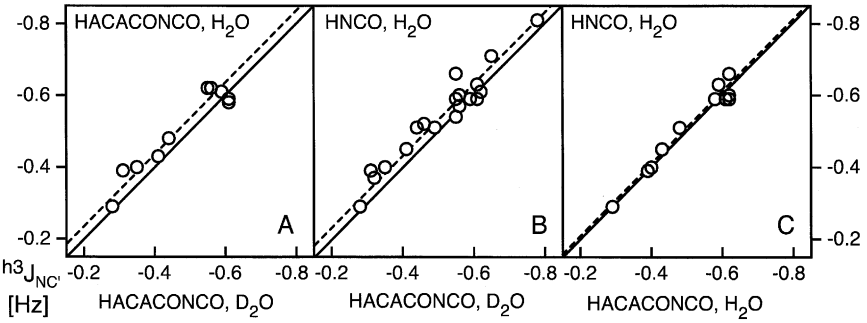

Figure 4. Comparison of $^{h3}J_{NC'}$ values obtained for deuterated and protonated H-bonds by different experiments indicated in Table 1. (A) HA(CACO)NCO in H_2O vs. HA(CACO)NCO in D_2O. (B) HNCO in H_2O vs. HA(CACO)NCO in D_2O. (C) HNCO in H_2O vs. HA(CACO)NCO in H_2O. Dashed lines correspond to the average differences between the respective data sets.

Table 1. List of trans-hydrogen/deuterium bond $^{h3}J_{NC'}$ values[a] determined in human ubiquitin

H^N	C′	$^{h3}J_{NC'}$ (D_2O)[b]	$^{h3}J_{NC'}$ (H_2O)[c]	$^{h3}J_{NC'}$ (H_2O, HNCO)[d]
3	15	-0.41 ± 0.01	-0.43 ± 0.01	-0.45
6	67	-0.61 ± 0.02	-0.58 ± 0.02	-0.59
7	11	-0.56 ± 0.03	nd[e]	-0.57
13	5	-0.65 ± 0.00	nd[e]	-0.71
15	3	-0.56 ± 0.01	-0.62 ± 0.07	-0.60
17	1	-0.55 ± 0.00	nd[e]	-0.54
23	54	-0.55 ± 0.04	nd[e]	-0.54
27	23	-0.44 ± 0.07	-0.48 ± 0.06	-0.51
30	26	-0.32 ± 0.02	nd[e]	-0.37
31	27	-0.35 ± 0.03	-0.40 ± 0.02	-0.40
32	28	-0.28 ± 0.02	> -0.29[f]	-0.29
42	70	-0.49 ± 0.02	nd[e]	-0.51
44	68	-0.55 ± 0.00	-0.62 ± 0.04	-0.59
50	43	-0.62 ± 0.01	nd[e]	-0.61
57	19	-0.31 ± 0.01	-0.39 ± 0.06	-0.39
64	2	-0.78 ± 0.00	nd[e]	-0.81
67	4	-0.55 ± 0.02	-0.62 ± 0.03	-0.66
68	44	-0.61 ± 0.02	-0.59 ± 0.02	-0.63
69	6	-0.46 ± 0.03	nd[e]	-0.52
70	42	-0.59 ± 0.01	-0.61 ± 0.00	-0.59

[a] All values are given in Hz. Errors represent standard deviations from two independently carried out experiments.
[b] $^{h3}J_{NC'}$ values are obtained from the HA(CACO)NCO experiment carried out at 1%/99% H_2O/D_2O, 35 °C.
[c] $^{h3}J_{NC'}$ values are obtained from the HA(CACO)NCO experiment carried out at 95%/5% H_2O/D_2O, 35 °C.
[d] $^{h3}J_{NC'}$ values are linearly intrapolated from values reported at 25 and 45 °C obtained at 95%/5% H_2O/D_2O, pH 6.5 by the long-range quantitative HNCO experiment (Cordier and Grzesiek, 2002).
[e] No $^{h3}J_{NC'}$ values could be determined due to overlap with the not completely suppressed water resonance.
[f] No cross peak above the noise threshold was detected. An upper bound for $|^{h3}J_{NC'}|$ was determined from the noise threshold value and the intensity of the reference peak.

$$^1J_{NC'}(k, k-1) + 2.74\ ^{h3}J_{NC'}(k, m) - 0.88\ ^{h3}J_{NC'}(n, k-1) + 15.6\ \text{Hz} = 0, \quad (1)$$

where k, m, n indicate the residue numbers of the respective N and C′ nuclei.

It was therefore of interest to examine whether the H/D exchange leads to detectable changes in the $^1J_{NC'}$ values. Figure 5A shows the $^1J_{NC'}$ couplings determined by the quantitative HA(CA)CO(N) experiment for ubiquitin in 5% D_2O/95% H_2O. As noticed before (Juranic et al., 1995), there is a dependency of the size of $^1J_{NC'}$ on the secondary structure, with $^1J_{NC'}$ values of about -15 Hz in α-helical and β-sheet conformations, and stronger (more negative) $^1J_{NC'}$ values in turn configurations (Figure 5A). Upon H/D exchange, a further shift to more negative $^1J_{NC'}$ values (i.e. a strengthening of $^1J_{NC'}$) can be observed. The strengthening has an almost linear dependence on the D_2O content (data not shown). Figure 5B shows the difference $\Delta^1J_{NC'}(^{2/1}H^N) = {}^1J_{NC'}(^2H^N) - {}^1J_{NC'}(^1H^N)$ obtained for the change from 5%/95% to 99%/1% D_2O/H_2O for all observed residues in ubiquitin. The isotope effect is quite uniform over the entire protein sequence. Exceptions are the prolines where only small changes are observed due to absence of the amide hydrogen. The all-residue-average of $\Delta^1J_{NC'}(^{2/1}H^N)$ amounts to -0.25 ± 0.07 Hz in ubiquitin (excluding values for prolines). A similar average change of -0.30 ± 0.16 Hz was observed for the similar sized human Y-box protein YB1 (data not shown).

It is interesting to compare the isotope effects on $^{h3}J_{NC'}$ and $^1J_{NC'}$ to the $^{h3}J_{NC'}/^1J_{NC'}$ correlation given by Equation 1. This correlation implies that all other things being equal, changes in $^{h3}J_{NC'}$ should be about -1.86 ($= 0.88$–2.74) times smaller than changes in $^1J_{NC'}$. Thus the observed average strengthening in

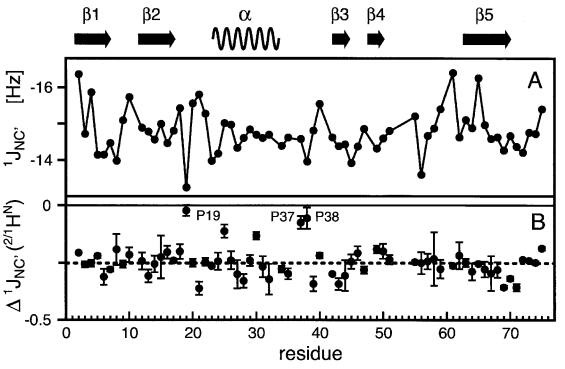

Figure 5. $^{2/1}H^N$ isotope effect on $^1J_{NC'}$ coupling constants. A: $^1J_{NC'}$ couplings obtained by the quantitative HA(CA)CO(N) experiment on a sample of ubiquitin in 95% H_2O/5% D_2O. Secondary structure elements of ubiquitin are indicated. B: difference $\Delta^1J_{NC'}(^{2/1}H^N) = {}^1J_{NC'}(^2H^N) - {}^1J_{NC'}(^1H^N)$ obtained from the data shown in (A) and from a second experiment carried out in 1% H_2O/99% D_2O. The average of $\Delta^1J_{NC'}(^{2/1}H^N)$ excluding prolines is shown as a dashed line.

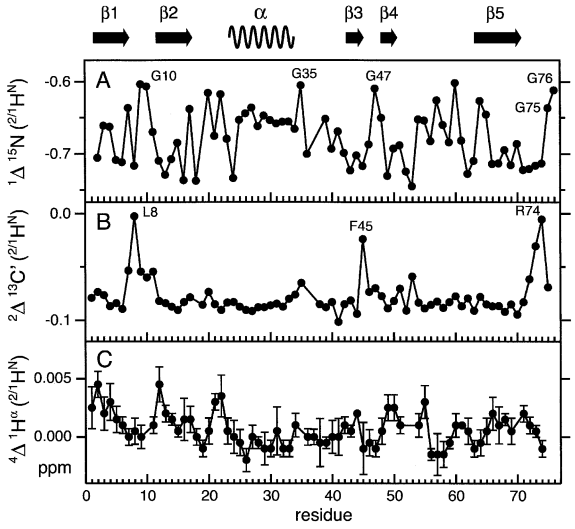

Figure 6. $^{2/1}H^N$ isotope effect on ^{15}N and $^{13}C'$ chemical shifts. Data were obtained from a 3D HA(CA)CON on a sample of ubiquitin in 50% H_2O/50% D_2O. Secondary structure elements of ubiquitin are indicated. A: $^1\Delta^{15}N(^{2/1}H^N)$ isotope shifts. B: $^2\Delta^{13}C'(^{2/1}H^N)$ isotope shifts. C: $^4\Delta^1H^\alpha(^{2/1}H^N)$ isotope shifts. Statistical errors in the isotope shifts are on the order of few ppb and are only shown for $^4\Delta^1H^\alpha(^{2/1}H^N)$.

$^1J_{NC'}$ couplings of 0.25 Hz would imply an expected average weakening in $^{h3}J_{NC'}$ couplings of 0.13 Hz for deuterated H-bonds. Clearly, the observed change of 0.03 ± 0.03 Hz for $^{h3}J_{NC'}$ is not consistent with this value expected from the relation in Equation 1. The reason for this is unclear, but it appears that Equation 1 is not applicable for estimating correlations between the $^1J_{NC'}$ and $^{h3}J_{NC'}$ isotope effects.

Amide H/D isotope effects on amide ^{15}N and $^{13}C'$ chemical shifts

Since the chemical shift of the amide ^{15}N and carbonyl $^{13}C'$ nuclei should be a reporter on the behavior of electronic wavefunctions in the peptide bond, we have also determined the respective isotope effects on these nuclei resulting from amide H/D exchange. The one-bond amide $^1\Delta^{15}N(^{2/1}H^N)$ and two-bond carbonyl $^2\Delta^{13}C'(^{2/1}H^N)$ isotope shifts were determined from a 3D HA(CA)CON experiment on a 50%D_2O/50%H_2O ubiquitin sample as the frequency differences of crosspeaks corresponding to the deuterated or protonated amide nitrogen.

Figure 6A shows the $^1\Delta^{15}N(^{2/1}H^N)$ isotope shifts as a function of residue number with values ranging from -0.6 to -0.75 ppm. Within ubiquitin's α-helix, $^1\Delta^{15}N(^{2/1}H^N)$ adopts quite uniform values of about -0.65 ppm, whereas more negative shifts of about -0.7 ppm are observed for most residues in β-sheet conformations. Since the derivative of the shielding surface, dσ/dr, is usually negative (Jameson, 1996), the negative $^1\Delta^{15}N(^{2/1}H^N)$ values indicate a shortening of the N-hydron bond length upon $^1H^N/^2H^N$ exchange. In some cases, correlations between one-bond isotope shifts and chemical shifts have been observed in chemically related compounds (Jameson, 1996). Thus, assuming similar isotope displacements, the steepness of the shielding surface is often correlated to the shielding σ itself. This is also evident for the $^1\Delta^{15}N(^{2/1}H^N)$ isotope shifts: glycine residues, which have upfield shifted ^{15}N resonances, i.e., increased ^{15}N shieldings, show the smallest absolute size $^1\Delta^{15}N(^{2/1}H^N)$ isotope shifts (Figure 6A). Considering all residues, a reasonable linear correlation can be found between $^1\Delta^{15}N(^{2/1}H^N)$ and $\delta^{15}N$ (Figure 7A). A linear fit yields

$$^1\Delta^{15}N(^{2/1}H^N) = -0.00487\,\delta^{15}N - 0.0940\ \text{ppm} \quad (2)$$

with a correlation coefficient $r = 0.72$ ($N = 68$). The correlation can be improved by including $^{h3}J_{NC'}$ (H-bond to the nitrogen atom of the peptide group) as a second linear parameter for residues where $^{h3}J_{NC'}$ has been determined. Figure 7B shows a comparison between a linear fit for these residues including only $\delta^{15}N$ or also $^{h3}J_{NC'}$. In the case of the double linear fit, the regression yields

$$^1\Delta^{15}N(^{2/1}H^N) = -0.00406\,\delta^{15}N - 0.0678\,{}^{h3}J_{NC'} - 0.149\ \text{ppm} \quad (3)$$

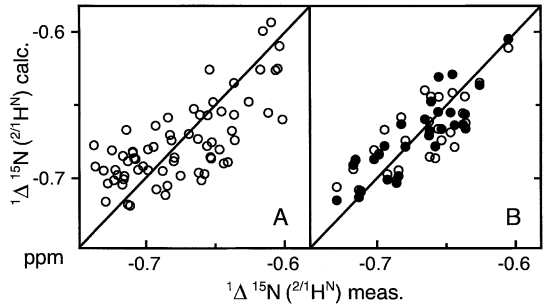

Figure 7. Linear regressions of $^1\Delta^{15}N(^{2/1}H^N)$ isotope shifts, ^{15}N chemical shifts ($\delta^{15}N$) and $^{h3}J_{NC'}$ coupling constants. A: $^1\Delta^{15}N(^{2/1}H^N)$ isotope shifts calculated from a linear correlation to $\delta^{15}N$ against measured values. B: $^1\Delta^{15}N(^{2/1}H^N)$ isotope shifts calculated from a linear correlation to $\delta^{15}N$ (open circles) and from a double linear correlation to $\delta^{15}N$ and $^{h3}J_{NC'}$ (filled circles) against measured values. See text.

with a correlation coefficient r = 0.85 (N = 29). The F-value (ratio of the chisquare difference between linear and double linear fit relative to the reduced chisquare of the double linear fit) is 8.55. Therefore, the improvement is to 99.3% significant according to the F-test criterion (Bevington and Robinson, 1992). Thus, it is clear that the $^1\Delta^{15}N(^{2/1}H^N)$ isotope shift is correlated with $^{h3}J_{NC'}$ and therefore with the H-bond donor-acceptor overlap. No significant correlations were found when values for $^1J_{NC'}$ or $^{h3}J_{NC'}$ from the H-bonds to the carbonyl oxygen were included into the linear fit.

The one-bond $^1\Delta^{15}N(^{2/1}H^N)$ isotope shifts result in a large separation of the 3D HA(CA)CON crosspeaks corresponding to deuterated or protonated amide groups. This makes it possible to determine the two-bond $^{2/1}H^N$ isotope shift of the $^{13}C'$ nucleus from the same two crosspeaks. Figure 6B shows the $^2\Delta^{13}C'(^{2/1}H^N)$ isotope shifts obtained as the $^{13}C'$ chemical shift differences of the amide deuterated or protonated HA(CA)CON crosspeaks. With the exception of several loop regions, the $^2\Delta^{13}C'(^{2/1}H^N)$ isotope shifts are quite uniform with values around −0.08 ppm. This observation is consistent with values reported by Tuchsen and Hansen (1991) on slowly exchanging H-bonds in BPTI. Similar to the $^1\Delta^{15}N(^{2/1}H^N)$ shifts, the negative $^2\Delta^{13}C'(^{2/1}H^N)$ values give evidence for an increased shielding of the $^{13}C'$ nucleus upon amide H/D exchange. Noted exceptions from this uniform behavior are β-turn residues T7-G10, F45, and the C-terminal, flexible residues R72-G75. For these residues, significantly reduced two-bond $^2\Delta^{13}C'(^{2/1}H^N)$ isotope shifts are observed (Figure 6B). Very likely, this reduction is due to the increased hydrogen exchange rates observed for these residues (Cordier and Grzesiek, 2002). The exchange rates are of similar size as the $^2\Delta^{13}C'(^{2/1}H^N)$ frequency separation and therefore lead to an averaging of the two isotopomer frequencies and a consequent reduction of the apparent isotope shift. This explanation is supported by the observation of significant line broadening in the $^{13}C'$ dimension for these residues.

In principle, the separation of the 3D HA(CA)CON crosspeaks by the large $^1\Delta^{15}N(^{2/1}H^N)$ isotope shifts can also be used to determine the $^4\Delta^1H^\alpha(^{2/1}H^N)$ isotope shifts with high precision and sensitivity. The values vary between 5 ppb and −2 ppb with a certain correlation to secondary structure (Figure 6C).

Discussion

In the present work we have studied the $^2H^N/^1H^N$ isotope effect on $^{h3}J_{NC'}$ and $^1J_{NC'}$ couplings as well as on ^{15}N, $^{13}C'$, and $^1H^\alpha$ chemical shifts. The results show that amide deuteration induces a very slight weakening of 0.03 ± 0.03 Hz for the $^{h3}J_{NC'}$ couplings, whereas the $^1J_{NC'}$ couplings are strengthened by 0.25 ± 0.07 Hz. In addition, the peptide group ^{15}N and $^{13}C'$ nuclei have increased shieldings, i.e. upfield shifts of about 0.65 ppm and 0.08 ppm, respectively. The isotope effect on the $^{h3}J_{NC'}$ couplings is consistent with a recent study on a limited number of H-bonds in double-stranded DNA (Kojima et al., 2000). In the latter case, the $^2H^N/^1H^N$ isotope exchange reduces the larger $^{h2}J_{NN}$ couplings (∼7 Hz) by about 0.3–0.4 Hz. Thus, the relative change of H-bond couplings upon deuteration is of similar order (5–10%) in proteins and nucleic acids.

According to the Born–Oppenheimer approximation, electronic wavefunctions are separable from the nuclear wavefunctions, and electronic behavior can be calculated with nuclear positions being treated as parameters. Thus there is no mass dependency per se of the electronic wave functions and molecular electronic properties such as nuclear shielding or scalar couplings. The isotope effects are rather the result of a different averaging of these electronic properties over the various nuclear positions that are accessible to the molecule due to zero-point and thermal motions. The mass difference of the isotopes leads to different kinetic energies and thus to different nuclear trajectories over which the electronic properties are being averaged. For the case of the $^2H^N/^1H^N$ isotope effects, it is obvious that the anharmonicity of the bond potential and the larger deuteron mass leads

to a decrease of the average $^2H^N$-N distance as compared to the $^1H^N$-N distance. This in turn corresponds to higher electron density within the N-hydron bond and probably also within the peptide bond. The observed increase in shielding for ^{15}N and $^{13}C'$, and the concomitant strengthening of $^1J_{NC'}$ are consistent with this notion.

Whereas the $^2H^N/^1H^N$ isotope effects on the ^{15}N and $^{13}C'$ shieldings and on the $^1J_{NC'}$ couplings are understandable from the different averaging of the $^2H^N$ and $^1H^N$ nuclear positions, within the context of a protein, the isotope effect on $^{h3}J_{NC'}$ also involves motions of the acceptor that could be influenced by other than local effects, e.g. isotope effects from nearby H-bonds or solvation.

In the following an attempt is made to use the isotope effect on the $^{h3}J_{NC'}$ couplings in order to estimate the change in H-bond donor-acceptor distance and the Ubbelohde effect in proteins. The observed weakening of the H-bond couplings is consistent with an average decrease of the donor-acceptor overlap by 0.02 ± 0.02 Å in deuterated protein H-bonds. It is interesting to compare this finding to $^2H^N/^1H^N$ isotope effects in crystallographic structures. Data of sufficient resolution on proteins are very limited. A comparison of a recent room temperature (298 K) neutron diffraction structure of amide-deuterated myoglobin (PDB code 1L2K, Engler et al., 2003) to a room temperature (287 K) x-ray structure of amide protonated myoglobin (PDB code1BZ6, Kachalova et al., 1999) yields an average increase of N-O distances in backbone H-bonds of 0.03 ± 0.06 Å for the amide-deuterated myoglobin. An increase of similar order (0.015–0.017 Å) upon hydrogen/deuterium exchange was found for the donor-acceptor distances in intermolecular O-H$\cdots$O hydrogen bonds of the small crystalline compound sodium hydrogen bis(4-nitrophenoxide) dihydrate (Kreevoy and Young, 1999).

Since $^{h3}J_{NC'}$ couplings are a measure of the overlap of hydrogen and oxygen acceptor orbitals in H-bonds (Barfield et al., 2001; Barfield, 2002), the changes in $^{h3}J_{NC'}$ couplings will not only depend on changes of the donor-acceptor N-O distances, but also on changes of the covalent N-hydron bond lengths. The neutron diffraction study of myoglobin (Engler et al., 2003) determined average amide N-D bond lengths of 0.98 Å. Due to the unfavorable scattering properties of H_2O, neutron diffraction studies are usually carried out in D_2O solvent and the current PDB entries do not contain N-H distances of high precision from neutron diffraction. Average N-H bond lengths in the hydrogen atom refined 0.54 Å resolution X-ray structure of crambin at 100 K (PDB code 1EJG, Jelsch et al., 2000) are 1.01 Å. Thus, the observed change in N-H vs. N-D bond lengths in protein crystallographic studies is about 0.03 Å. This is of similar size as typical isotope effects of about 0.02 Å observed for the covalent N-H or C-H bond lengths in small polyatomic molecules (see e.g., Jameson and Osten, 1984).

If both the lengthening of the N-O distance and the shortening of the N-hydron distance contribute additively, one would expect an increase of about 0.04–0.06 Å in the hydrogen-acceptor distance upon hydrogen/deuterium exchange in a protein backbone H-bond. Considering the crudeness of the assumptions, the neglect of other effects, such as an increase in the nitrogen/hydrogen orbital overlap, angular changes, and the limited precision of both structural and $^{h3}J_{NC'}$ data, this estimate does not seem inconsistent with the average decrease in hydrogen-acceptor distance of 0.02 ± 0.02 Å derived from the $^{h3}J_{NC'}$ couplings. However, it should be stressed that due to the large statistical scatter, the current data only provide a certain limit on the size of the Ubbelohde effect in proteins. It is also very likely that other intramolecular interactions in proteins hinder the relaxation to the full equilibrium geometry of protonated or deuterated H-bonds. Thus this situation is somewhat different from the intermolecular H-bonds of small crystalline molecules where this equilibrium is achieved more easily.

The small size of Ubbelohde effects should not mislead to underestimate their energetic importance. This is evident from the following estimate of the electrostatic energy of the H-bonds in proteins. Assuming partial elementary charges of -0.44 (N), 0.16 (H), -0.18 (O), and 0.32 (C′) determined from the ultrahigh resolution structure of crambin (Jelsch et al., 2000) and distances $d_{NH} = 1.01$ Å, $d_{NO} = 2.87$ Å, $d_{CO} = 1.23$ Å in a typical H-bond with linear geometry, a dielectric constant of 2 for the H-bonded protein interior, the cross H-bond part of the Coulomb energy as given by $E_{HO} + E_{HC} + E_{NO} + E_{NC}$ ($E_{ij} = q_i q_j/(\varepsilon d_{ij})$) amounts to -938 cal/mol. If H-bond deuteration leads to an increase by 0.03 Å in d_{NO} and a decrease by 0.03 Å in d_{NH} distances, the electrostatic attraction is reduced to -916 cal/mol. Thus deuteration would destabilize such an H-bond by 22 cal/mol. This very crude estimate is in quite reasonable agreement with a value of 9 cal/mol determined in a recent study of helical H-bonds (Krantz et al., 2002). Usually the free energy differences between

folded and unfolded states of proteins are small, e.g., 3–4 kcal/mol were observed for CspA and RNaseH (Jaravine et al., 2000). Therefore, deuteration of all H-bonds in a protein could lead to considerable differences in the total internal energy relative to the stabilization of the folded state.

Acknowledgements

We thank Prof Michael Barfield and the referees for many valuable comments on the manuscript and Marco Rogowski and Klara Rathgeb-Szabo for expert preparation of the isotope labeled proteins. This work was supported by SNF grant 31-61'757.00 to S.G.

Supporting Information Available

Tables of $^{1}J_{NC'}$ values, ^{15}N, $^{13}C'$, and $^{1}H^{\alpha}$ chemical shifts in ubiquitin for protonated and deuterated H-bonds (PDF). This material is available free of charge via the Internet at http://www.kluweronline.com/issn/0925-2738

References

Barfield, M. (2002) *J. Am. Chem. Soc.*, **124**, 4158–4168.
Barfield, M., Dingley, A.J., Feigon, J. and Grzesiek, S. (2001) *J. Am. Chem. Soc.*, **123**, 4014–4022.
Bax, A., Vuister, G.W., Grzesiek, S., Delaglio, F., Wang, A.C., Tschudin, R. and Zhu, G. (1994) *Meth. Enzymol.*, **239**, 79–105.
Benedict, H., Limbach, H.-H., Wehlan, M., Fehlhammer, W.-P., Golubev, N.S. and Janoschek, R. (1998) *J. Am. Chem. Soc.*, **120**, 2939–2950.
Bevington, P.R. and Robinson, D.K. (1992) *Data Reduction and Error Analysis for the Physical Sciences*, WCB/McGraw-Hill, Boston.
Cordier, F. and Grzesiek, S. (1999) *J. Am. Chem. Soc.*, **121**, 1601–1602.
Cordier, F. and Grzesiek, S. (2002) *J. Mol. Biol.*, **317**, 739–752.
Cornilescu, G., Hu, J.-S. and Bax, A. (1999a) *J. Am. Chem. Soc.*, **121**, 2949–2950.
Cornilescu, G., Ramirez, B.E., Frank, M.K., Clore, G.M., Gronenborn, A.M. and Bax, A. (1999b) *J. Am. Chem. Soc.*, **121**, 6275–6279.
Dingley, A. and Grzesiek, S. (1998) *J. Am. Chem. Soc.*, **120**, 8293–8297.
Englander, J.J., Del Mar, C., Li, W., Englander, S.W., Kim, J.S., Stranz, D.D., Hamuro, Y. and Woods, Jr. V.L. (2003) *Proc. Natl. Acad. Sci. USA*, **100**, 7057–7062.
Englander, S.W., Sosnick, T.R., Englander, J.J. and Mayne, L. (1996) *Curr. Opin. Struct. Biol.*, **6**, 18–23.
Engler, N., Ostermann, A., Niimura, N. and Parak, F.G. (2003) *Proc. Natl. Acad. Sci. USA*, **100**, 10243–10248.
Gombler, W. (1982) *J. Am. Chem. Soc.*, **104**, 6616–6620.
Grzesiek, S., Anglister, J., Ren, H. and Bax, A. (1993) *J. Am. Chem. Soc.*, **115**, 4369–4370.
Hansen, P.E. (1988) *Prog. Nucl. Magn. Reson. Spectrosc.*, **20**, 207–255.
Harris, C.M., Pollegioni, L. and Ghisla, S. (2001) *Eur. J. Biochem.*, **268**, 5504–5520.
Hvidt, A. and Nielsen, S.O. (1966) *Adv. Protein Chem.*, **21**, 287–386.
Ikura, M., Kay, L.E. and Bax, A. (1990) *Biochemistry*, **29**, 4659–4667.
Jameson, C.J. (1996) *Encyclopedia of Nuclear Magnetic Resonance*. D.M. Grant and R.K. Harris (Eds.). **4**, 2638–2655.
Jameson, C.J. and Osten, H.J. (1984) *J. Chem. Phys.*, **81**, 4300–4305.
Jaravine, V.A., Rathgeb-Szabo, K. and Alexandrescu, A.T. (2000) *Protein Sci.*, **9**, 290–301.
Jelsch, C., Teeter, M.M., Lamzin, V., Pichon-Pesme, V., Blessing, R.H. and Lecomte, C. (2000) *Proc. Natl. Acad. Sci. USA*, **97**, 3171–3176.
Juranic, N. and Macura, S. (2001) *J. Am. Chem. Soc.*, **123**, 4099–4100.
Juranic, N., Ilich, P.K. and Macura, S. (1995) *J. Am. Chem. Soc.*, **117**, 405–410.
Kachalova, G.S., Popov, A.N. and Bartunik, H.D. (1999) *Science*, **284**, 473–476.
Kojima, C., Ono, A. and Kainosho, M. (2000) *J. Biomol. NMR*, **18**, 269–277.
Krantz, B.A., Srivastava, A.K., Nauli, S., Baker, D., Sauer, R.T. and Sosnick, T.R. (2002) *Nat. Struct. Biol.*, **9**, 458–463.
Kreevoy, M.M. and Young, Jr. V.G., (1999) *Can. J. Chem.*, **77**, 733–737.
Legon, A.C. and Millen, D.J. (1988) *Chem. Phys. Lett.*, **147**, 484–489.
LeMaster, D.M. and Richards, F.M. (1988) *Biochemistry*, **27**, 142–150.
Makhatadze, G.I., Clore, G.M. and Gronenborn, A.M. (1995) *Nat. Struct. Biol.*, **2**, 852–855.
Markley, J.L., Putter, I. and Jardetzky, O. (1968) *Science*, **161**, 1249–1251.
Mittermaier, A. and Kay, L.E. (2002) *J. Biomol. NMR*, **23**, 35–45.
Pervushin, K., Ono, A., Fernandez, C., Szyperski, T., Kainosho, M. and Wüthrich, K. (1998) *Proc. Natl. Acad. Sci. USA*, **95**, 14147–14151.
Rosen, M.K., Gardner, K.H., Willis, R.C., Parris, W.E., Pawson, T. and Kay, L.E. (1996) *J. Mol. Biol.*, **263**, 627–636.
Salzmann, M., Pervushin, K., Wider, G., Senn, H. and Wüthrich, K. (2000) *J. Am. Chem. Soc.*, **122**, 7543–7548.
Scheurer, C. and Brüschweiler, R. (1999) *J. Am. Chem. Soc.*, **121**, 8661–8662.
Shenderovich, I.G., Smirnov, S.N., Denisov, G.S., Gindin, V.A., Golubev, N.S., Dunger, A., Reibke, R., Kirpekar, S., Malkina, O.L. and Limbach, H.-H. (1998) *Ber. Bunsenges. Phys. Chem.*, **102**, 422–428.
Shu, F., Ramakrishnan, V. and Schoenborn, B.P. (2000) *Proc. Natl. Acad. Sci. USA*, **97**, 3872–3877.
Smirnov, S.N., Golubev, N.S., Denisov, G.S., Benedict, H., Schah-Mohammedi, P. and Limbach, H.H. (1996) *J. Am. Chem. Soc.*, **118**, 4094–4101.
Sokolov, N.D. and Savel'ev, V.A. (1994) *Chem. Phys.*, **181**, 305–317.
Torchia, D.A., Sparks, S.W. and Bax, A. (1988) *J. Am. Chem. Soc.*, **110**, 2320–2321.
Tuchsen, E. and Hansen, P.E. (1991) *Int. J. Biol. Macromol.*, **13**, 2–8.
Ubbelohde, A.R. and Gallagher, K.J. (1955) *Acta Crystallogr.*, **8**, 71–83.
Wang, A.C., Grzesiek, S., Tschudin, R., Lodi, P.J. and Bax, A. (1995) *J. Biomol. NMR*, **5**, 376–382.